Materials and Design 92 (2016) 268-280
http://dx.doi.org/10.1016/j.matdes.2015.12.009

Enhancement of Process Capabilities in Electrically-assisted Double Sided Incremental Forming

D.K. Xu [a, b], B. Lu [a, c*], T.T. Cao [a], H. Zhang [a], J. Chen [a], H. Long [c], J. Cao [d]

[a] Department of Plasticity Technology, Shanghai Jiao Tong University, 1954 Huashan Road, Shanghai, 200030, P.R. China

[b] State Key Laboratory of Development and Application Technology of Automotive Steels (Baosteel), Shanghai, 201900, P.R. China

[c] Department of Mechanical Engineering, University of Sheffield, Sheffield, S1 3JD, UK

[d] Department of Mechanical Engineering, Northwestern University, Evanston, IL 60208-3111, USA

* Corresponding author, E-mail: binlu@sjtu.edu.cn

Abstract

Electrically-assisted incremental sheet forming (E-ISF) is an effective method to improve material formability by introducing the electric current in ISF process. This method is particularly useful for fabrication of conventional lightweight 'hard-to-form' materials such as magnesium and titanium alloys. However, the use of electricity and heat in the forming process may also introduce side effects to formed components, such as unsatisfied surface finish. In this work, an improved E-DSIF process has been developed by combining the double sided incremental forming (DSIF) and the electrically-assisted forming technology. Different types of forming tools and toolpath strategies are explored to improve surface finish and geometrical accuracy based on a customized DSIF machine. AZ31B magnesium alloy sheets are formed into a truncated cone shape to verify the proposed approaches. According to the comparative studies, the causes of the rough surface finish in the conventional E-ISF process are investigated, and the surface finish is refined by improving the contact condition at tool-sheet interface in the newly developed process. In addition, a hybrid toolpath strategy is proposed to further enhance the geometrical accuracy. The work demonstrates that the two challenging issues in the E-ISF process, surface finish and geometrical accuracy, could be improved by using the enhanced technologies.

Keywords

Double Sided Incremental Forming, Electric heating, Magnesium Alloy, Surface Finish, Geometrical Accuracy

Materials and Design 92 (2016) 268-280
http://dx.doi.org/10.1016/j.matdes.2015.12.009

1. Introduction

Incremental sheet forming (ISF) is an advanced flexible sheet forming technology. In this process, blank sheets are peripherally clamped, and locally deformed into various component shapes by using a stylus-type tool that follows pre-described toolpaths. Comparing to conventional sheet forming processes such as deep drawing, higher process flexibility and enhanced formability can be achieved in the ISF process. Moreover, the ISF process could potentially reduce the production lead time [1] and costs as well as energy consumption and environmental pollution [2, 3]. This technology is particularly suitable for manufacturing of small batched, high value-added, customized sheet components in automotive, aerospace and biomedical manufacturing sectors.

In recent years, the ISF process has attracted ever increasing interests from both academic and industrial communities. Varies of ISF processes have been developed, such is single point incremental forming (SPIF) [4], two-point incremental forming (TPIF) [5] and hybrid incremental forming [6]. These developed ISF technologies could overcome the challenges from the long forming time, uneven sheet thickness distribution and complex part geometry. However, due to the localized sheet deformation nature, the ISF process also faces other challenges, especially in fabrication of lightweight materials, such as limited formability, low geometric accuracy and rough surface finish. To overcome these problems, variants approaches have been developed to improve the formability, such as the multi-pass ISF [7] and double side incremental forming (DSIF) [8]. However, it is still difficult to process light weight 'hard-to-form' sheet metals at room temperature. A possible solution is to increase material formability by raising the forming temperatures. Consequently, different hot ISF methods have been developed and these approaches are summarized as follows:

Convection: Ji and Park [9] took advantage of heat convection by using hot air blowers to heat magnesium AZ31 sheets in the ISF process. Various forming temperatures have been employed and the experiment results show that the forming limit increased as the forming temperature elevated. However, they also found that it was difficult to accurate control the forming temperature by adopting hot air blowers as the heat source.

Conduction: Ambrogio et al. [10] developed a heating system for forming the AZ31 sheets in the ISF process. In this system, a heater band was mounted at the external surface of the fixture.

Materials and Design 92 (2016) 268-280
http://dx.doi.org/10.1016/j.matdes.2015.12.009

Other than the local heating approach, this technology has to globally heat the whole sheet during the forming process, which reduces the energy efficiency.

Radiation: Duflou et al. [11] proposed a laser-assisted ISF process. In this process, a laser beam is employed to locally heat the sheet. Göttmann et al. [12] also developed a hot ISF system by integrating a coaxial rotating optics to the ISF system. This laser-assisted ISF process has many advantages such as well controlled heating zone and temperature. However, the equipment cost is much higher comparing to other processes.

Friction heat: Otsu et al. [13] employed the frictional heat generated between the rotating tool and the static sheet to improve the material formability. Xu et al. [14] also investigated the influence of tool surface texturing on the formability in the frictional-stir ISF process. The friction assisted ISF approach is easy to implement. However, uncontrollable forming temperature and severe tool wear are two major challenges.

Electric heating: Fan et al. [15] proposed an electric hot incremental sheet forming (E-ISF) process. Ambrogio et al. [16] further investigated this approach by quantifying the heat supplement respecting to the forming parameters. Göttmann et al. [12] try to control the forming temperature by adjusting the input current. In the E-ISF process, surface finish and geometric accuracy are the two major problems due to the extreme high temperature at local area.

Combined electric heat and friction heat: Palumbo and Brandizzi [17] developed a process in which a static electricity heating was employed to pre-heat the sheets and localized friction heating was superimposed to further increase the temperature. A scaled automotive component in Ti6Al4V was successfully formed under an aimed temperature of 400 °C.

Comparing all the hot ISF approaches, the frictional-stir ISF and the E-ISF processes are more flexible with reduced equipment cost. However, E-ISF has wider process potentials than frictional-stir ISF because it is more efficient in heating, less dependent on component geometry and the temperature can be controlled by adjusting the input current [18]. Concerning the ISF researches, most of the E-ISF investigations were implemented based on the SPIF process. In SPIF, only one forming tool is employed, which only has limited process capability in further improving the existing problems. In recent years, the DSIF based E-ISF process, namely the electrically-assisted double side incremental sheet forming (E-DSIF), has been proposed. Cao et al [19] firstly proposed the combination of electricity-assisted forming and DSIF process. Meier and Magnus [20] presented a robot-based E-DSIF process, which demonstrated the feasibility of E-DSIF. Asgar et

Materials and Design 92 (2016) 268-280
http://dx.doi.org/10.1016/j.matdes.2015.12.009

al [21] employed the electric plus other than the direct current in the DSIF process and successfully fabricate the titanium alloys. Although the E-DSIF process shows great potential, there is limited investigation due to a series of challenges, such as the rough surface finish and inaccurate part geometry. In addition, slave tool and sheet may lose contact in the DSIF process [22, 23]. This becomes a seriously problem in E-DSIF as electric current cannot pass through the too-sheet interface when losing contact occurs.

Concerning the challenges from surface finish, although roller-ball tool [24] with improve lubricant [25] has been adopted for the cold ISF process, surface finish is still a challenge in E-ISF due to its high forming temperature. This is especially true for E-DSIF process as the involvement of tool squeezing would significantly increase the contact pressure and result even higher friction. In previous studies, some special lubricants, such as lubricant film of nickel matrix with molybdenum disulfide (MoS_2) self-lubricating material, were introduced to the E-SPIF process [26]. Another possible approach is the employment of coating technology. Zhang et al. [27] improved the lubricant condition by employing the Nano-$K_2Ti_4O_9$ whisker and the solid graphite powder-coated porous ceramic coating in the ISF process. Although the coating method is effective in reducing the tool-sheet friction, the surface preparation of blank sheet is time-consuming and not available for manufacturing large-scale components. Further studies are needed to explore the possible solutions for the E-DSIF surface finish.

Concerning the improvement of geometrical accuracy, Tekkeya et al [28] presented a surface reconstruction algorithm to minimize geometrical deviations. Macari et al [29] suggested a few strategies to improve the accuracy including use of a flexible support, application of a counter force, backdrawing incremental forming and use of optimized trajectories. Han et al [30] considered the residual stress as a major cause of ISF springback. Ruszkiewicz et al [31] investigated the effect of part stiffness on the springback. These studies on geometrical accuracy are majorly based on the cold ISF process. In E-SPIF, this is even more complex due to the involvement of thermal effects in the forming process. Shi et al. [19] recently fabricated low carbon steel DC04 with 0.8 mm sheet thickness into a pyramid part with higher geometrical accuracy as compared to the case without electric heating. An optimized helical toolpath was developed to avoid discharge phenomenon which may lead to earlier abnormal failure. Ruszkiewicz et al [32] studied the effect of direct electric current on springback. At the meantime, the investigations and

Materials and Design 92 (2016) 268-280
http://dx.doi.org/10.1016/j.matdes.2015.12.009

strategies on improving the geometric accuracy in the E-ISF is still limited, which is especially true for the advanced E-DSIF process.

The above literature studies summarize the E-DSIF challenges in both process implementation (such as losing contacts) and final part qualities of surface finish and geometric accuracy. Focusing on these challenges, this paper aims to enhance E-DSIF process capabilities through improving the contact condition, optimizing tool design/selection and developing novel forming strategies. In this work, an improved E-DSIF system has been developed to ensure stable tool-sheet contact. Based on this new system, the mechanism that causing the severe surface finish in the E-DSIF process is studied and the strategy to improve the surface finish has been proposed. In addition, the geometric errors in the E-DSIF process are quantified and a hybrid DSIF toolpath strategy is proposed to increase the geometric accuracy. Based on the experimental results, discussions on improving surface finish and decomposing geometrical errors are given. Conclusions are made for the developed reinforced E-DSIF system.

2. E-DSIF Experimental setup

2.1 E-DSIF principle and machine design

In the existing DSIF approach, industrial robots [8], hexapods [33], or in-house developed machines [22] have been employed to implement the DSIF process. The general concept of DSIF is shown in Fig. 1a, in which the sheet is deformed according to the motions of tools at both sides. However, conventional DSIF approaches rigidly control the displacement of both master and slave tools, which may result losing contact between tool and sheet as shown in Fig. 1b. This is because there will be gap between slave tool and sheet due to sheet thinning and tool deflections. This gap may not be well predicted and compensation of this gap becomes extremely difficult. Ensuring a steady and continues contact between tool and the sheet is a key point in the successfully implementation of the E-DISF process. To overcome this problem, in this work, an improved DSIF process has been developed as shown in Fig. 1c. In the new development, the slave tool is supported by an air cylinder, which acts as a spring to ensure the contact between the slave tool and sheet.

Materials and Design 92 (2016) 268-280
http://dx.doi.org/10.1016/j.matdes.2015.12.009

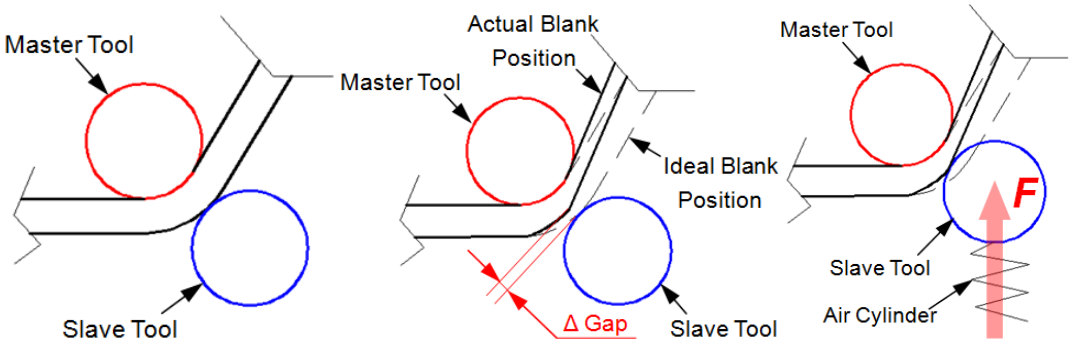

(b) (c) (d)

Fig. 1 Development of an improved E-DSIF process: (a) idea position of forming tools; (b) lose contact of slave tool under displacement control; (c) proposed approach to ensure a stable contact;

To implement the proposed principle, in this work, a horizontal DSIF machine with two forming tools at each side of blank sheet has been developed, as shown in Fig. 2a. In this machine, while the master tool is rigidly clamped and driven by the master XYZ linear motion unit, the slave tool is supported by an air cylinder to ensure the sheet and slave to contact. Fig. 2b shows the details design of the slave tool connected to an air cylinder. In the forming process, the sheet clamped on the sub frame will be deformed according to the movement of both tools.

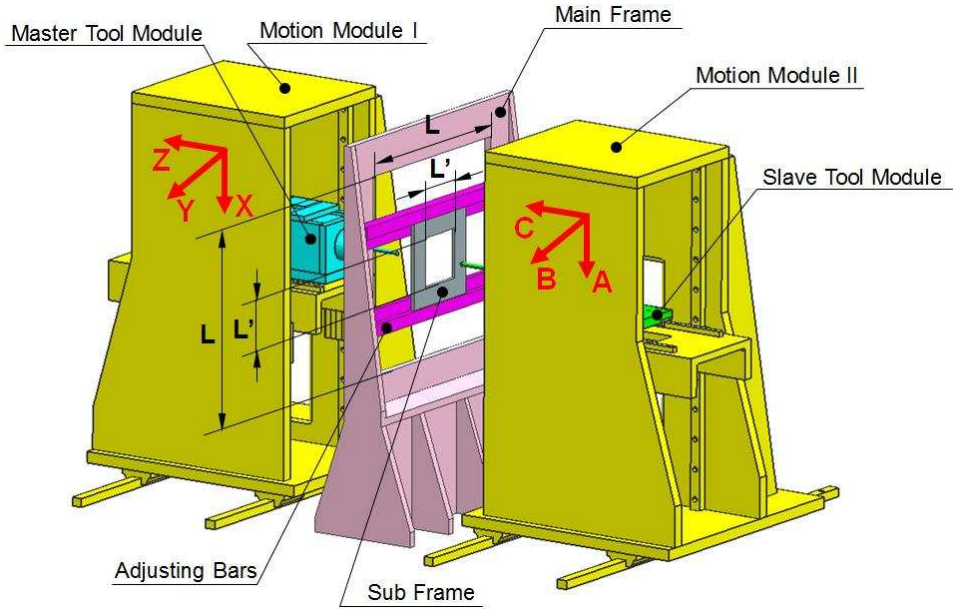

(a)

Materials and Design 92 (2016) 268-280
http://dx.doi.org/10.1016/j.matdes.2015.12.009

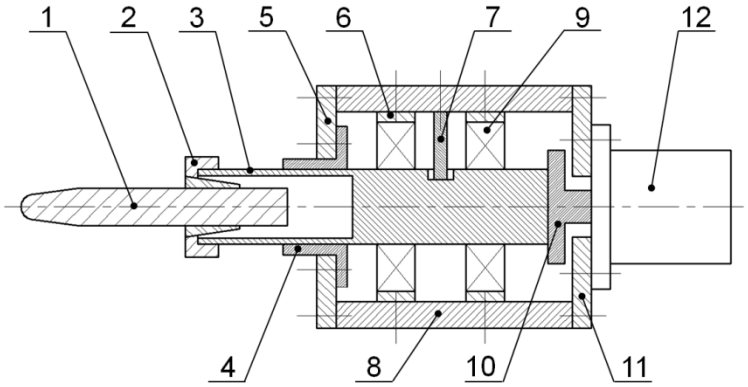

Fig. 2 Developed slave tool with air cylinder (1—slave forming tool, 2—collet, 3—cylindrical tool holder with positioning groove, 4—supporting flange, 5—front cover plate, 6—bearing chock, 7—positioning pin, 8—frame with two open ends, 9—bearing, 10—thrusting rod, 11—back cover plate, 12—air cylinder)

To achieve the E-DSIF process on the developed DSIF machine, varies of circuit connects may be employed as shown in Fig. 3. In previous study, the Mode II connection is usually employed [20, 21]. In Mode II, electric current pass through both tools to generate a local heat zone around the tool-sheet contact region. However, in this way, the electric current will heat both tool bodies as well. The higher tool temperature may result lower tool stiffness, which may increase the tool deflection under forming load. In this work, an alternative solution of Mode I is employed. In Mode I, the electric current will pass through slave tool but not the master tool. In this way, no electricity will pass the master tool and only the slave tool is acted as an electron.

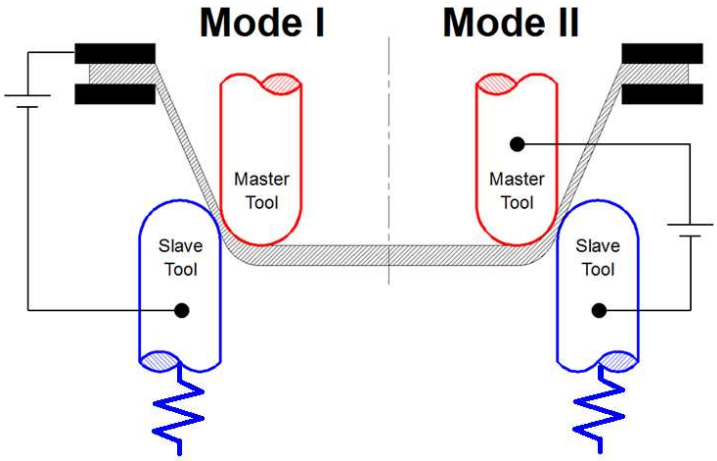

Fig. 3 Schematic of circuit connection in E-DSIF

Materials and Design 92 (2016) 268-280
http://dx.doi.org/10.1016/j.matdes.2015.12.009

Based on the proposed concept, the E-DSIF machine has been developed shown in Fig. 4. This machine employed a 6-Axis PC-based control system from Power Automation to ensure the synchronized motion of master and slave tools. In addition, a direct current (DC) power supply with maximum current of 800A and voltage of 15V has been utilized to input specified energy to heat the materials. Both circuit connection modes illustrated in Fig. 3 can be employed in the developed system. To reduce the tool oxidation, high temperature nickel alloy GH4169 was employed as tool material. In addition, a thermal camera was employed to monitor the sheet temperature. To obtain the correct temperature value, the temperature range was set to correct values in the thermal camera software and thermocouple was employed to calibrate the thermal cameral. During the calibration process, the emissivity was adjusted to match the temperatures obtained in thermocouple and thermal cameral. In this way, the emissivity parameter can be determined can be determined and the thermal cameral can be calibrated before ISF experiments.

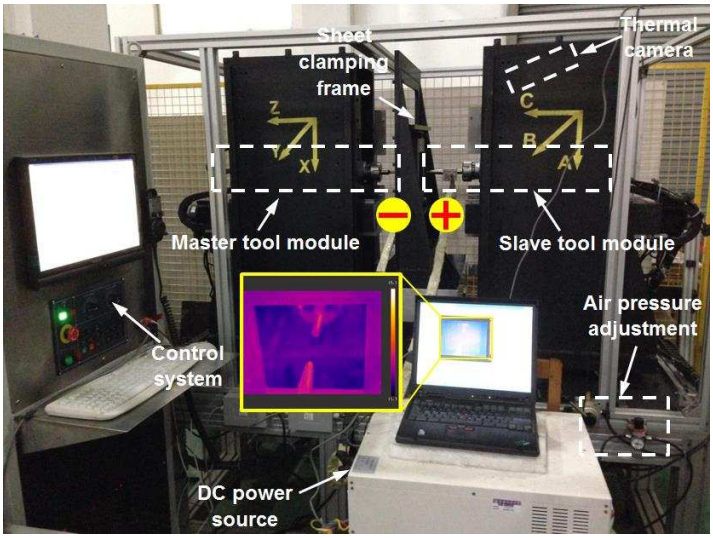

Fig. 4 Experimental setup of E-DSIF system

2.2 E-DSIF Toolpath

In the current study of the SPIF process, the forming tool follows a continuously helical path to deform the sheets from outside towards inside. To majors parameters, incremental depth ΔZ and scallop height S_h are employed to control the interval between adjacent helical paths as shown in Fig. 5. Compared to traditional contour toolpath, the adopted helical toolpath is able to avoid unexpected failure by eliminating the phenomenon of discharge in E-ISF, which also had been confirmed by Shi et al. [34]. Concerning the E-DSIF toolpath, as two tools are involved, a series

Materials and Design 92 (2016) 268-280
http://dx.doi.org/10.1016/j.matdes.2015.12.009

of point couples has to be generated to represent the positions of the both master tool and slave tool centers during the forming process. In this work, the master toolpath that expressed by a series of point will be generated first. In the master toolpath generation, contours have been generated base on the designed part by using the z-height slicing method. These contours have then interpolated to helical toolpaths. The technical details can be referring to the Malhotra's toolpath generation algorithm [35].

After generating the master toolpath, the corresponding position of slave tool can be determined by adjusting the vector between the centers of master and slave tools. As shown in Fig. 5, the distance $\mathbf{d}$ between the master and slave tool center can be obtained by:

$$\mathbf{d} = R_M + R_S + (1 - C_w)t_0 + C_w s t_0 \cos\alpha \tag{1}$$

where R_M and R_S are the radii of master and slave tools, respectively. t_0 is the initial sheet thickness, α ranging from 0° to 90^o is the wall angle of desired component at the contact point T, s is the squeezing factor ($0 < s \leq 1$), and C_w (=1 or 0) is a factor to determine whether the compensation of sheet thinning and squeezing are considered.

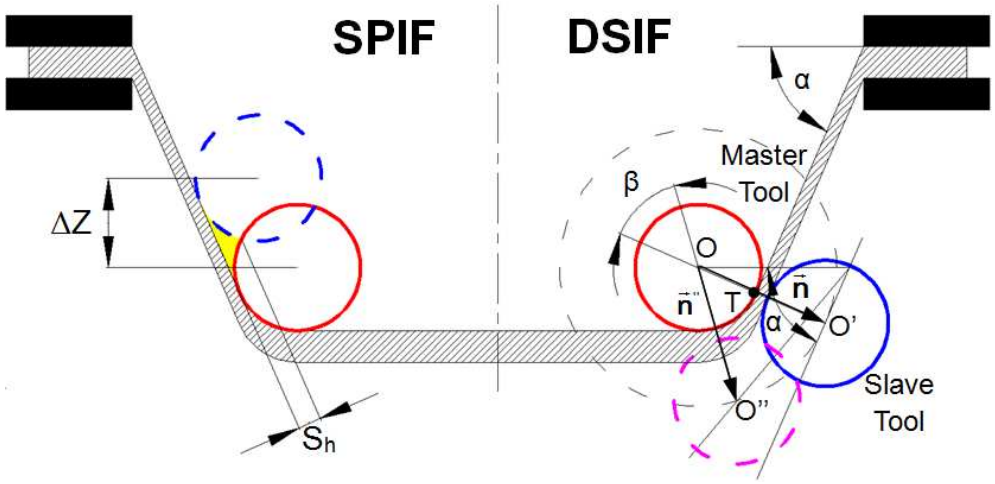

Fig. 5 Illustration of utilized toolpath strategies

In particular, three typical cases are listed as follows:

1. No compensation ($C_w = 0$). The distance between the master and slave tool can be calculated by $\mathbf{d} = R_M + R_S + t_0$;

Materials and Design 92 (2016) 268-280
http://dx.doi.org/10.1016/j.matdes.2015.12.009

2. Sheet thinning compensation ($C_w = 1$, $s = 1$). The distance is determined by $\mathbf{d} = R_M + R_S + t_0 \cos\alpha$. The predicted sheet thickness $t_0 \cos\alpha$ is obtained by sine law.
3. Sheet squeezing with different amounts ($C_w = 1, 0 < s < 1$). A certain amount of squeezing that the sheet will experience is decided by a constant s . Accordingly, the Eq. (1) changes its form to $\mathrm{d} = R_M + R_S + s t_0 \cos\alpha$.

With the calculated distance d, the position of slave tool can be obtained by employing the positions of master toolpath O and the normal at contact point $\vec{\mathbf{n}}$:

$$O' = O + \mathrm{d} \cdot \vec{\mathrm{n}} \tag{2}$$

where O and O' are the tools center position, which can be expressed by (O_x, O_y, O_z) and (O'_x, O'_y, O'_z) respectively. $\vec{\mathbf{n}}$ is a vector to represent the surface normal at the contact point, which can be expressed as (n_x, n_y, n_z).

To further enhance the capability of DSIF toolpath algorithm, a shifting angle β is proposed as shown in Fig. 5. The range of a shifting angle β is from 0 to α . Through this parameter a new normal vector $\vec{\mathbf{n}}''$ can be obtained by rotating the original $\vec{\mathbf{n}}$ by angle β. The component of $\vec{\mathbf{n}}''$ can be given by:

$$\begin{cases} n''_x = \dfrac{\sqrt{n_x^2 + n_y^2} \cdot \cos\beta + n_z \cdot \sin\beta}{\sqrt{n_x^2 + n_y^2}} n_x \\ n''_y = \dfrac{\sqrt{n_x^2 + n_y^2} \cdot \cos\beta + n_z \cdot \sin\beta}{\sqrt{n_x^2 + n_y^2}} n_y \\ n''_z = -\sqrt{n_x^2 + n_y^2} \cdot \sin\beta + n_z \cdot \cos\beta \end{cases} \tag{3}$$

Using the updated normal with the consideration of shifting angle β, the positions of slave toolpath O''_D can be calculated by:

$$O''_D = O_D + \mathrm{d} \cdot \vec{\mathrm{n}}'' \tag{4}$$

Materials and Design 92 (2016) 268-280
http://dx.doi.org/10.1016/j.matdes.2015.12.009

Using the above described approach, synchronized toolpaths can be obtained for the movement of master and slave tools.

2.3 The material and working temperature in the E-DSIF process

Thermal properties and electrical conductivity may have significant influence on the achieved temperature in the E-DSIF process. Materials such as aluminum alloys have low electric resistance, which require high electric current to achieve the working temperature. The high electric current may also generate heat in the tool, which significantly increases the tool temperature. In addition, heat capacity and thermal conductivity may also affect the temperature increasing rate and temperature distribution. In this work, a commonly used 'hard-to-form' material, magnesium alloy AZ31B has been employed. The specific heat capacity, thermal conductivity coefficient and resistance of the AZ31B are 1.13 J/g • °C, 83.9 W/(m • K) and 0.434 mΩ, respectively. Concerning the material deformation in the ISF process, plane strain and biaxial stretching are two major deformation modes [36]. During the ISF process, sheet materials experience complicated deformation such as through-thickness shear, bending, stretching and cyclic loading [37]. Accurate determination of ISF working temperature is difficult due to the complex material deformation behaviors. Considering material formability, the working temperature range is studied by revisiting previous research on hot ISF of AZ31 sheets. Ji and Park [9] successfully formed a circular cup with a wall angle of 59° at temperature 150 °C. Ambrogio et al. [10] found that 45° truncated cone could be formed without failure at 200 °C. Zhang et al. [38] systematically investigated the influence of anisotropy of the AZ31 sheets and observed the maximum formable wall angles of these materials were over 60° at 250 °C. Taleb et al. [39] suggested that the formability of AZ31 significantly increased at 200 °C but would not further improve at an even higher temperature of 250 °C. Sy and Nam [40] found that the maximum formable wall angle (75°) could be obtained at 250 °C. These works suggest that the working temperature of AZ31 is about 200 °C to 250 °C. In this work, the lower bound of 200°C is employed as the higher forming temperature may bring more side effects such as poor lubricant condition and scratches on the softened sheet surface

3 The E-DSIF Forming process

Materials and Design 92 (2016) 268-280
http://dx.doi.org/10.1016/j.matdes.2015.12.009

In this study, AZ31B sheet with 1.4 mm thickness was employed and a 45° truncated cone shape with an initial fillet of radius 10 mm (Fig. 6) was designed to evaluate the capability of E-DSIF in enhancing surface finish and geometrical accuracy of formed components.

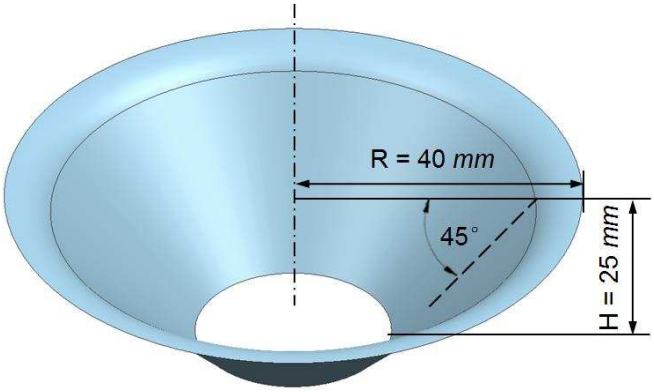

Fig. 6 A designed 45° truncated cone

In the E-DISF process, both master and slave tools as well as the sheet could be connected to form the electric circuit. However, if both tools are employed as the electrodes, heat will be concentrated at local forming area, which may cause excessive material softening. In this study, the circuit connection Mode I instead of Mode II (as shown in Fig. 1) was preferred to avoid the overheating. Table 1 shows the key process parameters used in the experiment. For both E-SPIF and E-DSIF, the feed rate was fixed as 800 mm/min, and no tool rotation was allowed throughout the forming process. To reduce the friction at the tool-sheet interface, ROCOL® copper based anti-seize compound was used to ensure better lubrication and conductivity between the forming tool and the sheet. The scallop height was fixed as 0.005 mm. In additional, the slave tool supported the sheets with a pre-set backing pressure of 0.1MPa during the forming process. This pressure would ensure the contact of slave tool and sheet but would not over squeeze the sheet. As shown in Fig. 7, the truncated cone components were formed by using both E-SPIF and E-DISF approaches with the process parameters listed in Table 1.

Table 1 Key process parameters of E-ISF

		E-SPIF	E-DSIF
Toolpath	Scallop height (mm)	0.005	0.005
	Thinning compensation C_w	No	No

Materials and Design 92 (2016) 268-280
http://dx.doi.org/10.1016/j.matdes.2015.12.009

	Squeezing factor s	No	No
	Shifting angle β (°)	No	0
	Backing pressure (MPa)	No	0.1
Feed rate (mm/min)	800		
Tool rotation speed (rpm)	0		
Tool radius (mm)	5		
Temperature range (°C)	200±10		
Lubricant	Copper based anti-seize compound		

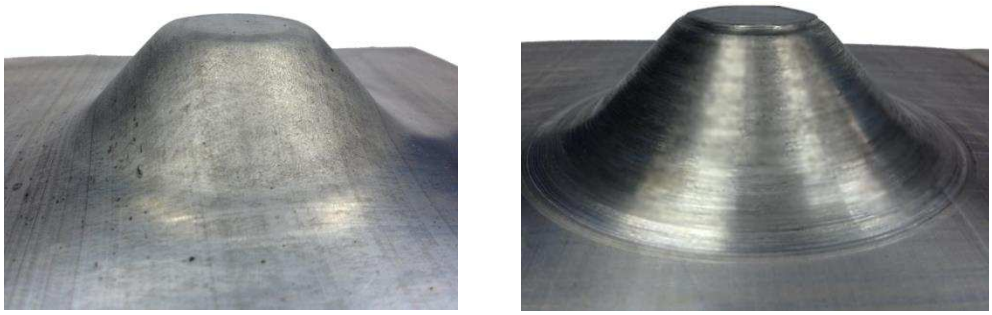

(a) (b)

Fig. 7 Formed 45° truncated cones: (a) E-SPIF and (b) E-DSIF

As both E-SPIF and E-DSIF are localized heating processes, the location of maximum sheet temperature changes in correspondence with the movement of the heat source. The typical temperature variation history for both E-SPIF and E-DSIF process is illustrated as shown in Fig. 8. As can be seen in the Figure, similar trends of temperature variation can be observed for the two processes. The maximum temperature gradually increases from room temperature to the target forming temperature of 200 °C in about 200s. After that the maximum temperature is maintained within the target range of 200±10 °C by manually adjusting the input current. Concerning the temperature distribution as shown in the top left corner, it can be observed that the temperature distribution is non-uniform, and the maximum temperature appears at the location where the forming tool contacts with the sheet. Considering the temperature variation at specific point, cyclic heat loading is observed as the monitored temperature oscillates at the specific location. When the tool approaches the region where the specific point locates, the temperature at the point periodically reaches its maximum value in every pass. When the tool moves away to a next location

Materials and Design 92 (2016) 268-280
http://dx.doi.org/10.1016/j.matdes.2015.12.009

after the temperature achieves its peak value of about 210 °C, the minimum temperature in the cycle can drop down to about 80 °C. This measurement suggests the unlike the single cycle of temperature raising and dropping in conventional hot stamping, cyclic temperature change exists in the E-ISF process due to its localized heating nature. In addition, this cyclic heat impact may results a different microstructure revolution in the forming process. As temperature rising up and drop down in very short period of time, there may not be sufficient time for recrystallization. However, further studies are needed to confirm this argument in the future.

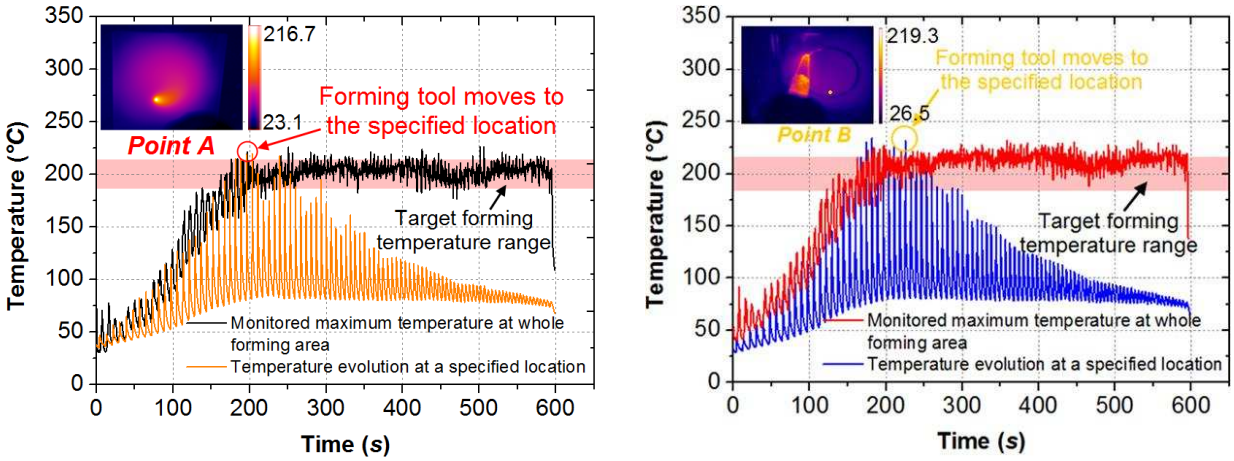

(a) (b)

Fig. 8 Monitored temperature of the sheet during forming process:(a) E-SPIF; (b)E-DSIF

4 The E-DSIF surface finish

4.1 Tool head designs and surface finish measurement

The preliminary study on temperature distribution suggests that maximum temperature occurs at the contact zone between sheet and the tool where the electricity applies. The high temperature and high contact pressure at the tool-sheet interface may cause scratches and result in rough surface finish. This low E-ISF surface quality has also been mentioned by Fan et al. [17]. To further investigate the surface finish issue in the E-ISF process, other than a rigid tool (RT) as shown in Fig. 9a, a roller-ball tool (RBT) (introduced by Kim and Park [27]) were employed in this work as shown in Fig. 9b. This design was organically employed in the cold ISF process to improve the surface finish. In this work, the capability of this RBT is explored in the E-DSIF process and the influence of surface finish from tool design can be evaluated at elevated temperature.

Materials and Design 92 (2016) 268-280
http://dx.doi.org/10.1016/j.matdes.2015.12.009

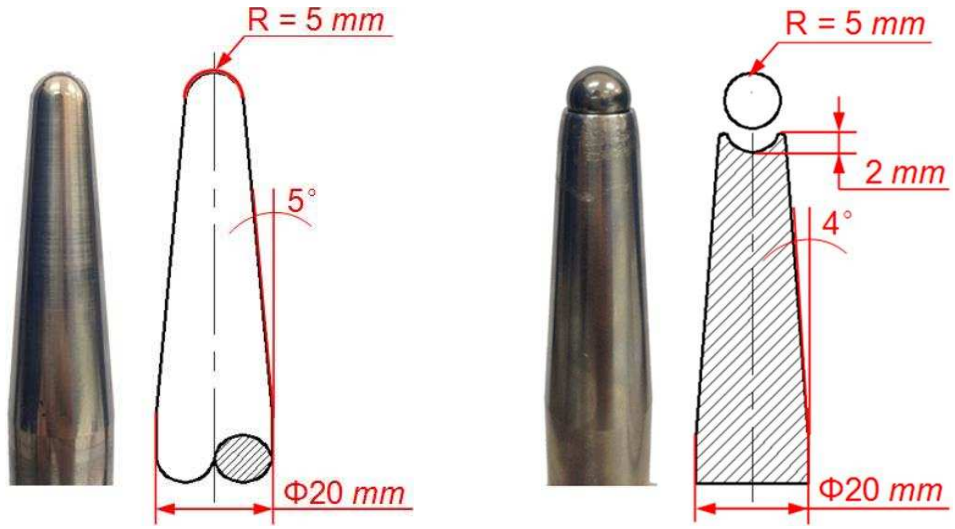

(a) (b)

Fig. 9 Different types of forming tools: (a) rigid tool (RT) and (b) roller-ball tool (RBT)

To examine the detailed surface finish on formed parts, BRUKER® ContourGT-I 3D optical microscope with a root mean square repeatability of 0.01nm has been employed. In the experiments, the 20x objective lens is employed to ensure the consistency of measurement result. Both inner and outer surfaces were measured and repeated in five equally spaced areas (0.58 mm by 0.43 mm). Arithmetic average of the 3D roughness S_a in Eq. (5) was calculated to quantitatively describe the surface finish.

$$S_a = \frac{1}{A}\iint_A |Z(x,y)|\,dxdy \tag{5}$$

where A is the area of measured region, $Z(x,y)$ denotes the values of peaks and valleys on the region.

Using the microscope and the described measurement approach, the surface topography in initial sheet is given in Fig. 10. As can be seen in the figure, the initial S_a value of the original sheet surface is 0.721μm, which indicates very good surface finish. This value is employed as a reference for the comparison between the formed parts in the following sections.

Materials and Design 92 (2016) 268-280
http://dx.doi.org/10.1016/j.matdes.2015.12.009

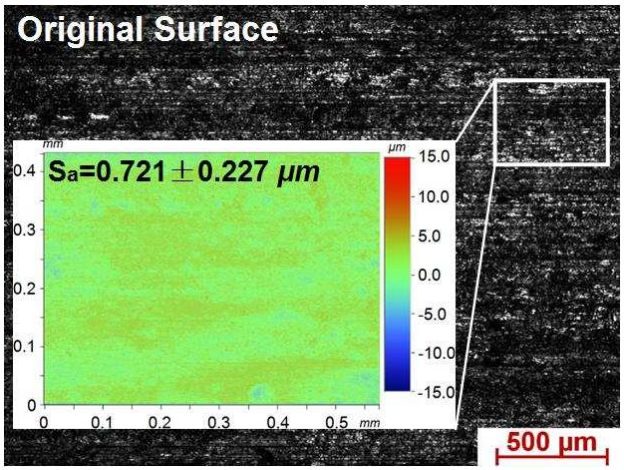

Fig. 10 Surface finish of original sheets

4.2 Investigation of surface finish in E-SPIF and E-DISF

Using the described approaches, the surface topography of E-SPIF and E-DSIF processes are compared as shown in Fig. 11 and 12. As shown in Fig. 11, notable tool marks and the phenomenon of 'orange peel' were detected at inner and outer surfaces of the component formed in E-SPIF. The corresponding S_a values with standard deviation are 1.595μm and 8.249μm, respectively. Comparing the inner surfaces between E-SPIF and E-DSIF, the one obtained by the roller-ball tool in E-DSIF is smoother with narrow and shallow tool marks (Fig. 12a), and its measured average S_a (0.941μm) decreases by 41.00%. Concerning the outside surfaces, the one obtained in E-DSIF (Fig. 10b) has a S_a value of 5.187μm, which is slightly improved comparing to the outside surface but not as good as the inner surface in E-SPIF. As shown in Fig. 12b, considerable tool marks caused by electric discharge can be observed. The result indicates that although the free rotation of the roller-ball tool is regarded as a major advantage in improving the surface finish in cold ISF process, it does not always work well in E-DSIF: when the roller-ball tool is also worked as an electrode, the sheet surface quality decreases due to the occurrence of electric discharge when the current pass between the rotating ball and the sheet.

Materials and Design 92 (2016) 268-280
http://dx.doi.org/10.1016/j.matdes.2015.12.009

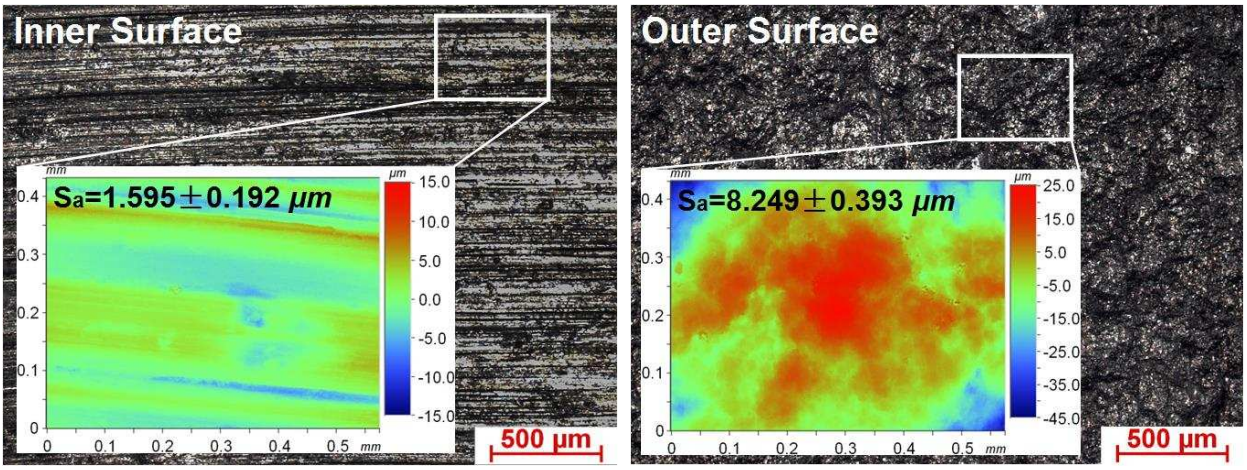

(a) (b)

Fig. 11 Surface finish of components formed in E-SPIF with rigid tool: (a) inner surface and (b) outer surface

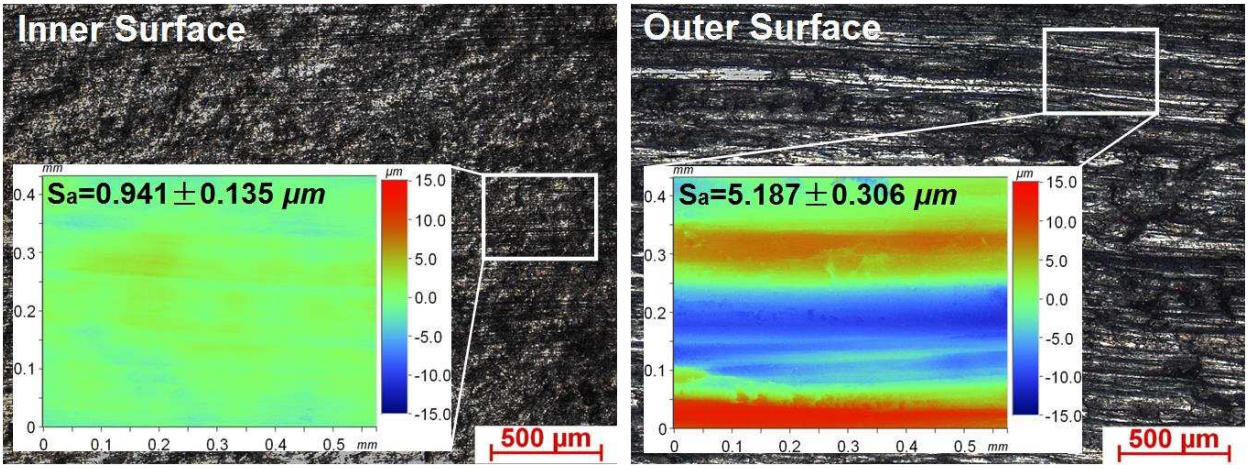

(a) (b)

Fig. 12 Surface finish of components formed in E-DSIF with two roller-ball tools: (a) inner surface and (b) outer surface

4.3 Elimination of discharge phenomenon

In order to eliminate the electric discharge, a rigid tool instead of the roller-ball tool was employed as the slave tool in E-DSIF. In the new experiment, no discharge phenomenon was observed during the whole forming process. The obtained inner surface (Fig. 13a) displayed the same topography as the one shown in Fig. 12a. Concerning the outer surface as shown in Fig. 13b, no electric discharge can be observed and a much lower S_a value of 1.381 μm can be obtained. The quality was improved by 73.4% as compared to the one processed by roller-ball tool.

Materials and Design 92 (2016) 268-280
http://dx.doi.org/10.1016/j.matdes.2015.12.009

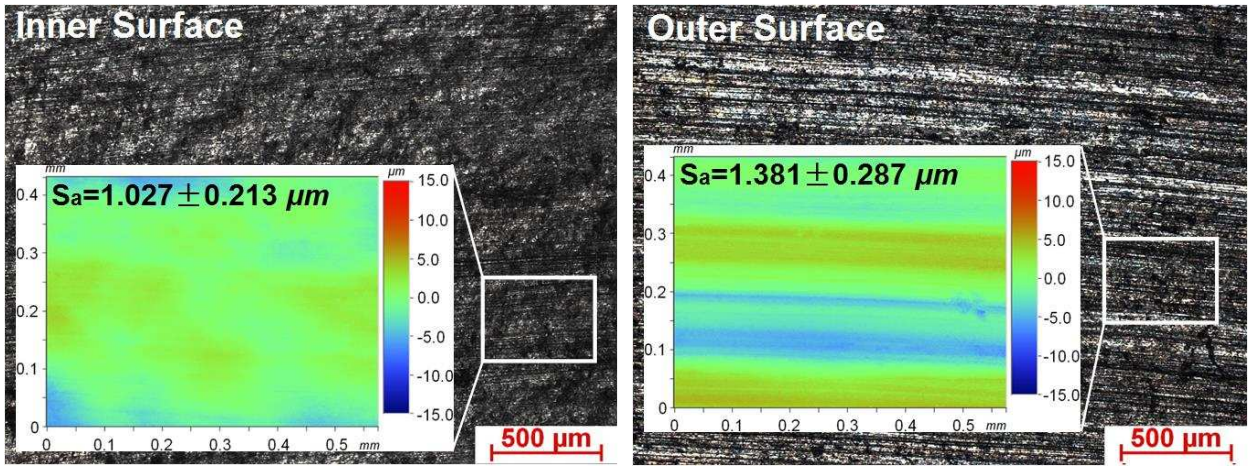

(a) (b)

Fig. 13 Surface finish of components formed in E-DSIF with roller-ball master tool and rigid slave tool: (a) inner surface and (b) outer surface

The above experimental results of surface finish suggest that employing the rigid tool as slave tool in the E-DSIF process has obvious advantages since the roller-ball tool may cause electric discharge. In those cases, to maintain the temperature of sheet at a certain level, current continuously passes into the sheet deformation area through the slave tool. As a result, regardless of what type of tool is used, the accumulated heat continuously raises the temperature of slave tool. This is confirmed by the monitored temperature of the slave tool as shown in Fig. 14, in which the temperature of slave tool continues to increase during the entire forming process. Therefore, the friction condition may be worsened when the temperature of forming tool is even higher than the sheet. In addition, the above result also suggests that although the rigid tool with sliding friction condition is employed, it will not cause the surface damage. This is because the slave tool does not take the major forming load and the corresponding contact pressure is much lower comparing to master tool.

Materials and Design 92 (2016) 268-280
http://dx.doi.org/10.1016/j.matdes.2015.12.009

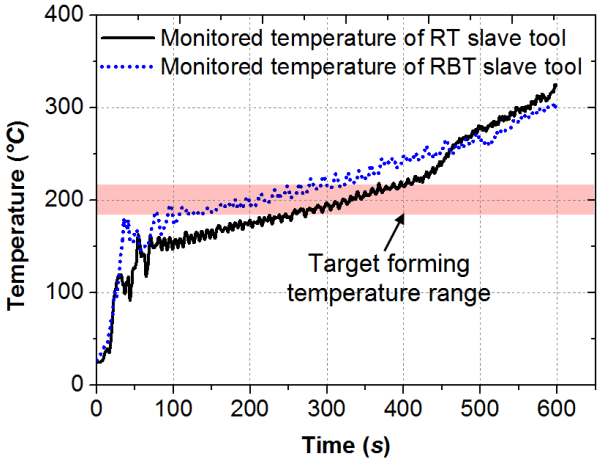

Fig. 14 The slave tool temperature during E-DSIF process (RT-Rigid tool and RBT-Roller-ball tool)

5 The E-DSIF geometrical accuracy

5.1 Investigation of geometrical accuracy in E-SPIF and E-DSIF

Geometric accuracy is another challenge in the ISF process. To examine the geometrical accuracy, the symmetric cross section of formed components was scanned by using KEYENCE® LK-G150 laser displacement sensor. The geometry of the formed components in E-SPIF and E-DSIF were compared to the nominal shape as shown in Fig. 15. It can be observed that before the components reached the depth of around 7.5 mm, the produced shapes matched well with the desired shape in both cases. However, after this depth, a significant geometrical deviation can be observed due to the bending effect at the initial forming stage. As compared with E-SPIF, the maximum geometrical deviation in E-DSIF is reduced by 29.8 %, from 3.2 mm to 2.2 mm. This reduction mainly attributes to the support from the slave tool at outer surface. Although E-DSIF shows an enhanced capability on geometrical accuracy, the deviation is still considerable large.

Materials and Design 92 (2016) 268-280
http://dx.doi.org/10.1016/j.matdes.2015.12.009

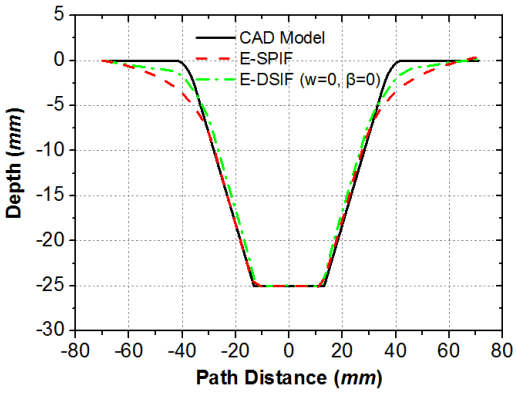

Fig. 15 Comparison of geometrical accuracy in E-SPIF and E-DSIF

5.2 A hybrid DSIF toolpath strategy

The result obtained in Fig. 16 suggests that the main shape deviation comes from the bending of sheet in the fillet area at the initial forming stage. This inaccuracy cannot be minimized by optimizing the forming parameters. Alternatively, direct modification of toolpath may have larger impact on the geometric accuracy. In this work, a hybrid DSIF toolpath strategy has been proposed as illustrated in Fig. 16. At the initial stage, the slave tool acts similarly as the role of a backing plate in SPIF process. Only the master tool will move downward while the slave tool will remain at the same level in Z direction. In this way, the fillet can be formed with minimized bending effect and the corresponding shape deviation will be reduced. After forming the fillet, the two tools will move down simultaneously as those in conventional DSIF process. Using this strategy, the geometrical deviation caused by the bending effect may be reduced while the advantages of DSIF such as squeezing effect can still be maintained.

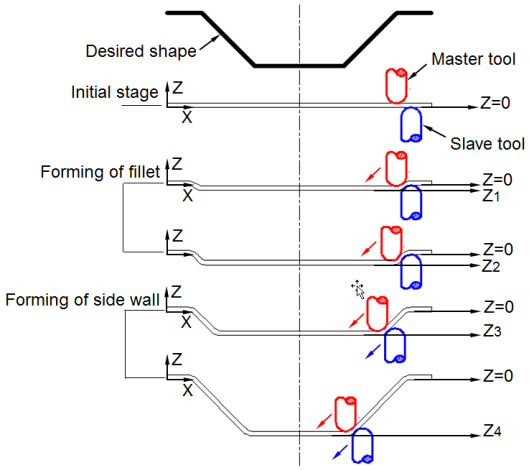

Fig. 16 Illustration of proposed hybrid DSIF toolpath strategy

Materials and Design 92 (2016) 268-280
http://dx.doi.org/10.1016/j.matdes.2015.12.009

The profile measurement in Fig. 17 confirmed that a more accurate geometry can be obtained by using the proposed hybrid DSIF toolpath strategy as compared to the one formed by using conventional DSIF toolpath strategy. The maximum shape deviation decreased by 30.16%, from 2.2 mm to 1.5 mm. In addition, it can also be observed that the maximum shape deviation did not occur at the region of side wall, but transferred to the flat surface of the formed component. A region with bulges was detected as shown in the figure. This phenomenon attributes to the higher backing pressure imposed onto the sheet by the slave tool during forming the fillet. The solution was to reduce the backing pressure as 0MPa in the forming of fillet, and then increase to the normal value in forming the inclined wall. Through this adjustment the bugle height reduced from 1.6 mm to 0.4 mm. The maximum geometrical inaccuracy at the side wall was 1.4 mm which was only 60.9% of the value obtained by using the conventional toolpath strategy.

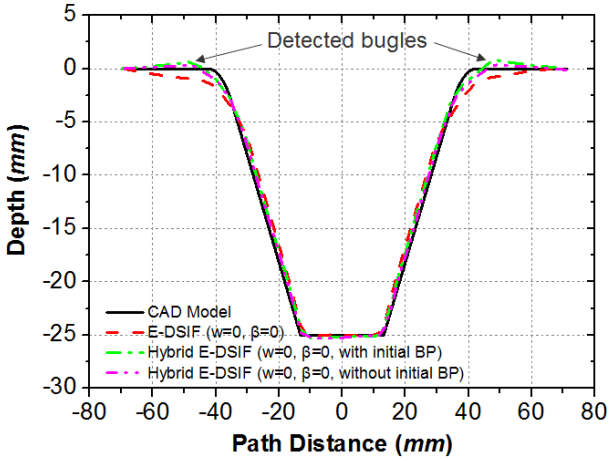

Fig. 17 Improved geometrical accuracy by using hybrid DSIF toolpath strategy

5.3 Geometric error quantification

The results demonstrate the E-DSIF process provides an enhanced geometrical accuracy. However, after unclamping and trimming, springback may also occur due to the release of residual stress. To further investigate the geometric deviations, the truncated cone parts fabricated by the E-SPIF process, the E-DSIF process and the Hybrid E-DSIF process have been measured after forming, unclamping and trimming stages. Fig. 18 compares the profiles of the parts after different states. As can be seen in Fig. 18b, the E-SPIF part shows the largest springback after unclamping, while those for both E-DSIF and Hybrid E-DSIF are much smaller. After trimming of flange, the parts continue to springback as shown in Fig. 18c. At the final state, the Hybrid E-DSIF parts suggested the smallest geometric deviation of about 1.0 mm comparing to the designed shape while

Materials and Design 92 (2016) 268-280
http://dx.doi.org/10.1016/j.matdes.2015.12.009

the E-DSIF part turns out to be the worst, with a maximum deviation of about 2.0 mm. The springback of the E-SPIF part turns out to have positive effect in this case: although this part is worst after forming, the consequence springback during unclamping and trimming reduced the overall geometric error, the maximum deviation reduced from original 3.0 mm to about 1.7 mm in the final state.

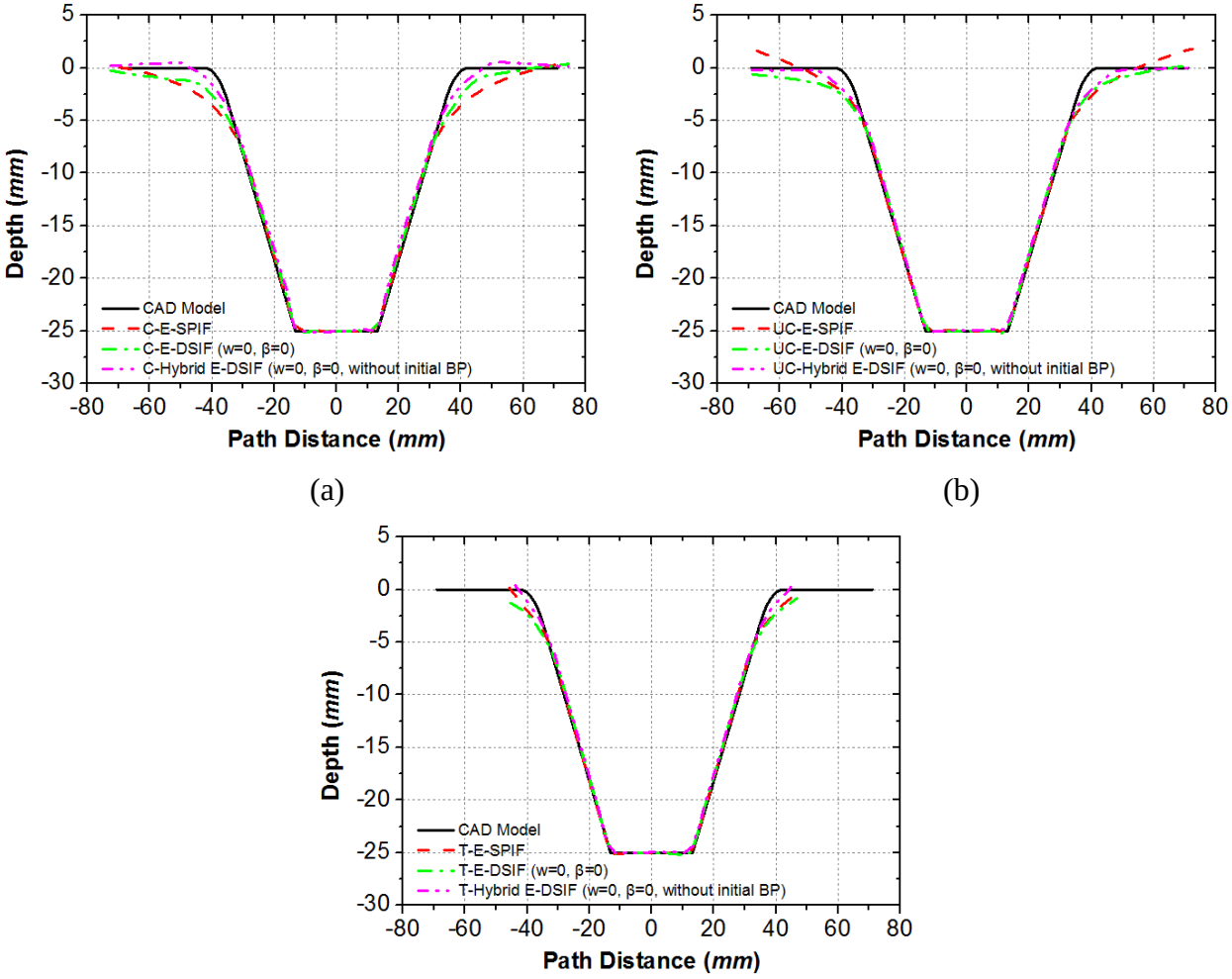

Fig. 18 Measured cross section profile of formed components: (a) before unclamping (b) after unclamping and (c) after trimming

To further investigate the geometric accuracy, the final geometric error (δ_{final}) may be considered as a sum of shape deviations generated in forming, unclamping and trimming, which can be expressed as:

$$\delta_{final} = \delta_c + \delta_{uc} + \delta_t \tag{4}$$

Materials and Design 92 (2016) 268-280
http://dx.doi.org/10.1016/j.matdes.2015.12.009

where δ_c is the error measured when the formed components were still clamped on the frame, δ_{uc} and δ_t are the geometrical errors obtained from unclamping and trimming, respectively.

Using the measured profiles in Fig. 18, the geometric errors of δ_c, δ_{uc} and δ_t in each step can be obtained, as shown in Fig. 19. As can be seen in Fig. 19a, after forming process, the E-SPIF process has the maximum error of over 3 mm, while that for E-DSIF is about 2 mm and that for Hybrid E-DSIF strategy is 1 mm. In the unclamping stage as shown in Fig. 19b, E-SPIF part has the largest springback of more than 1mm while the springback for both E-DSIF and Hybrid E-DSIF parts are less than 0.5 mm. In the trimming process as shown in Fig. 19c, similar to previous process, the E-SPIF part has the largest springback. The smallest springback comes from the E-DSIF part, where almost no springback can be observed in the trimming process. The final geometrical error is shown in Fig. 19d. For the E-SPIF part, as the springback in the unclamping and trimming processes occur at the opposite direction of the initial error, the initial maximum error was compensated by the springback and leaded to a reduced geometric error. For the E-DSIF part, as there is only limited springback in the unclamping and trimming process, the maximum final geometric error value is almost unchanged. Similarly, for the Hybrid E-DSIF part, the springback is limited and the maximum final geometric error value is almost slightly reduced to about 1 mm. This result not only confirms the improved geometric accuracy in the Hybrid E-DSIF process, but also provides a clear understanding on the geometric deviation in both E-SPIF and E-DSIF processes.

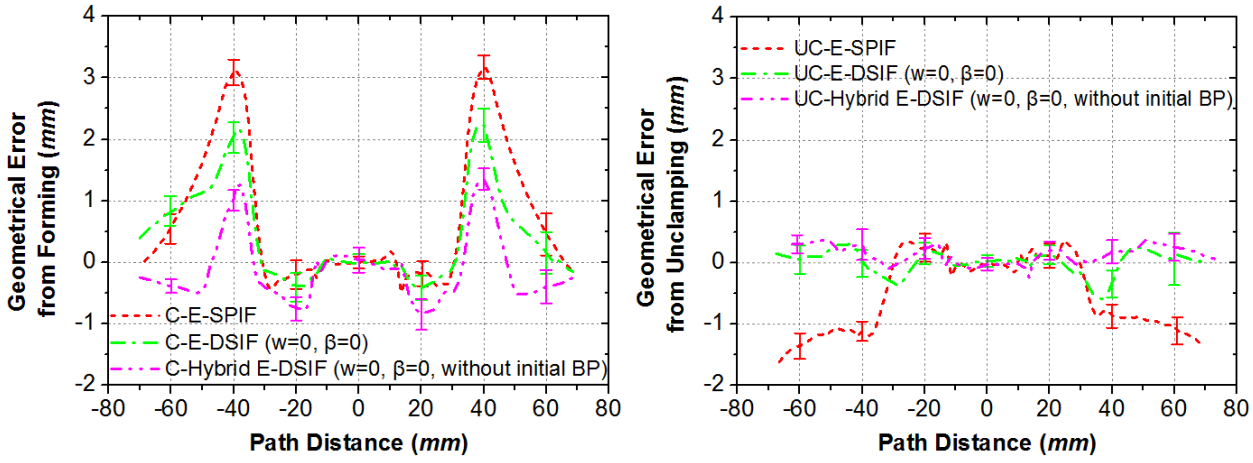

(a) (b)

Materials and Design 92 (2016) 268-280
http://dx.doi.org/10.1016/j.matdes.2015.12.009

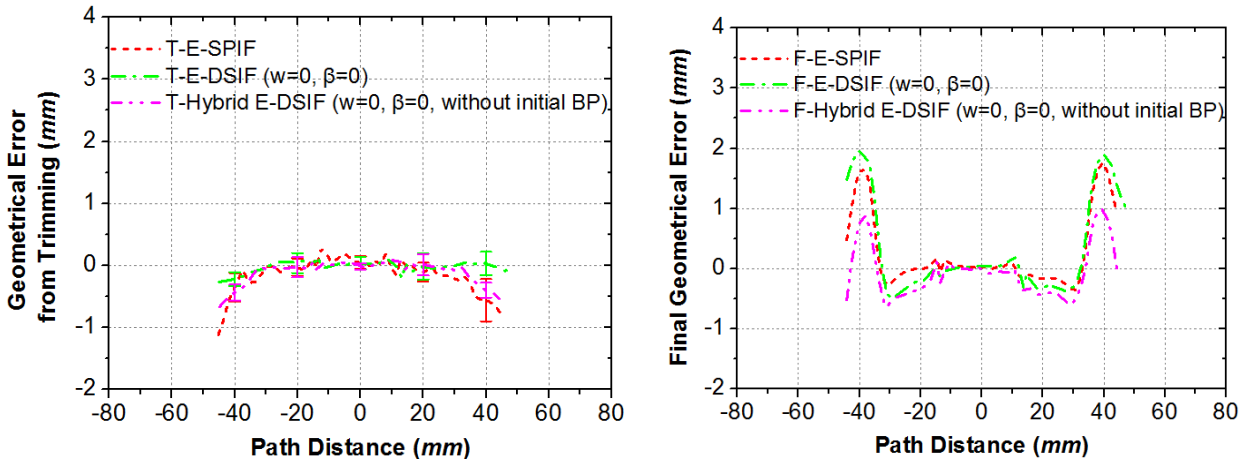

(c) (d)

Fig. 19 Decomposition of shape deviation: (a) δ_c (b) δ_{uc} (c) δ_t and (d) δ_{final}

6 Discussion

6.1 The E-DSIF process

This work introduced an E-DSIF process for fabrication of hard-to-form materials by combining the double side incremental forming and the electrical-assisted heating method. The investigation conducted in this work reveal the complexity of E-DSIF process: The two tools will squeeze the sheet during forming process, which produces the squeezing effect. At one side, the squeezing effect would increase the compressive hydrostatic stress resulting in higher formability, and suppress the orange peel effect; on the other side, high contact stress may result in severe friction problem. This may be especially true when introducing the electric heat in which materials are softened under elevated temperature condition. Another notable effect is from the localized heating, cyclic thermal loading can be observed and the temperature varies all the time, which lead to even more complex material deformation behaviors.

The cyclic thermal loading and the squeezing effect in the E-DSIF are the two major differences comparing to conventional ISF processes. Although the thermal and the squeeze effects benefit the successful forming of AZ31 sheet with considerable geometric accuracy, the combined factors may also lead to bad surface finish and even tool damage. To overcome these problems, different forming strategies have been proposed including the selection of forming tools with corresponding current circuit connection and the hybrid forming approaches. Improved understandings are obtained during the investigation of the E-DSIF process.

Materials and Design 92 (2016) 268-280
http://dx.doi.org/10.1016/j.matdes.2015.12.009

Comparing to the conventional E-SPIF process, the two-tool approach in the E-DSIF process has some advantages: the backing plate becomes unnecessary and the springback turns out to be smaller due to a different sheet deformation mode. Comparing to other heating methods such as laser assisted incremental forming, the equipment cost is much lower and the sheet can be heated at the same time as deformation without complex optical system. However, the E-DSIF method may be more suitable for materials with larger electrical resistance. Although material such as aluminum alloys can also be formed by using this approach, larger electrical current is required to heat up the sheet which is not energy efficient.

6.2 The E-DSIF Surface finish

Similar to the E-SPIF method, one challenges of the E-DSIF method is the surface finish. The squeezing effect and high contact pressure make it even worse. Solutions including improving the lubricant, such as lubricant film of nickel matrix with molybdenum disulfide (MoS_2) self-lubricating material [26]. However, this will increase the process complexity and pretreatment on sheet has to be performed before forming. Non-contact heating method such as laser may partly reduce this problem as the tool can be stay cooled to reduce the adhesion of material. For the E-ISF process, the electric current will pass and heat the tool. To overcome this problem, different forming tools and strategies have been employed to look for a solution. It was found that although the utilization of roller-ball tool is usually considered as a feasible way to improve the surface finish in ISF process, this research concludes that it cannot serve as an electrode because of the electric discharge due to unsteady contact. The electric discharge and the unsteady contact may be caused by following reasons:

- The high temperature causes severe friction condition due to the evaporation of the grease in the lubricant.
- Due to the uneven temperature and uneven thermal expansion, the dimension of ball may not fit the dimension of ball cap, which cause an unstable rotation condition. This was observed in the experiments.
- The unstable rotation of ball may result an unstable contact between tool and sheet, which result the electric discharge.

In addition, the roller-ball tool is employed in this work is based on the conventional design. This design may only take limited horizontal load. When fabricating parts with larger wall angles,

Materials and Design 92 (2016) 268-280
http://dx.doi.org/10.1016/j.matdes.2015.12.009

larger horizontal load may occur and the design concept of obsolete roller-ball tool may be used to overcome this problem [41].

This study suggests that the rigid tool is a more suitable option when the load is not too high. The rigid tool could keep a stable contact condition between tool and sheet under high temperature. In the E-SPIF process, as only one tool has to serve as both forming tool and electrode, high contact pressure and high temperature occur at the same point, which may reduce the surface quality and cause severe tool wear. In addition, 'orange peel' can be observed at outer surface of component, which results in rough surface topography. This effect can be avoided in E-DSIF by exerting pressure on the surface through the slave tool.

The E-DSIF process employs two forming tools to achieve better surface finish on both sides of component surface. In this way, separating the tool functions of taking forming load and serving as electric become feasible. Concerning the circuit connection (Fig. 3), the investigation result suggests that Mode I is a better option in E-DSIF than Mode II. This is because in the Mode II current will pass and heat both tools and Mode I could avoid undesirable heat concentration on sheet and overheating of forming tools. Under Mode I connection, the roller-ball tool is employed as the master tool since it remains at a relatively low temperature with good contact during the forming. The rigid tool can be employed as the slave tool due to its good ability in maintaining a stable contact between tool and sheet. In this way, better surface finish can be obtained using the circuit connection and tool strategy. It is also worthwhile to note that there are also other modes with different combination of electric circuit connections and counter loads. This would result different sheet deformation behavior due to the change of stress state and forming temperature. Further study is needed to fully explore the effects from electric connection and counter forces.

6.3 The E-DSIF Geometrical accuracy

Concerning the geometrical accuracy, the E-DSIF process provides greater possibilities in enhancing geometrical accuracy than the E-SPIF process. As the relative position between the master and slave forming tools can be varied, it offers higher degrees of flexibility in sheet deformation. In this work, the slave tool travels only in the horizontal direction without the downward movement and acts as a moving backing plate to suppress the geometrical deviation resulted from bending. After the forming of fillet, both forming tools will move down simultaneously as those in conventional DSIF process. In this way, the hybrid toolpath not only

Materials and Design 92 (2016) 268-280
http://dx.doi.org/10.1016/j.matdes.2015.12.009

reduces the bending effect, but also takes the advantages of DSIF. It is worth mentioning that the backing pressure supplied by the air cylinder will also affect the geometrical accuracy. At the initial stage, the sheet has only limited stiffness. Lower backing pressure may be used to prevent the over bending of sheet. Subsequently, the backing pressure could be increased to normal value when the forming of fillet is completed to ensure the stable contact between tool and sheet. In addition, other type of tool path strategies such as a feature-based flexible toolpath strategy proposed by Lu et al. [42] may also be introduced in the E-DISF process in the future, which will make positive contributions in improvement of geometrical accuracy.

Concerning the source of geometric error, the error generated in the forming stage takes the largest percentage in this truncated cone case, reaches a maximum value of 3 mm in the E-SPIF case. The springback from unclamping could reach 1.5 mm while that from trimming is about 1mm. Although the springback may be varied depending on the shape and the stiffness of the final part, the measurement suggests that the geometric deviation generated in forming plays a major role and minimizing this error would significantly benefit the overall geometric accuracy at the final stage. Another possible error source of E-DSIF is thermal expansion, due to the uneven temperature distribution and cyclic heating as shown in Fig. 8, the sheet was undergoing cyclic expansion and contraction during the forming process. This may result even more complex geometric deviation and increased the residual stress. However, the experiment results in this work don't suggest significant geometric deviations due to thermal expansion. This may be because the forming temperature is not too high thus this effect is not obvious. Forming of titanium alloy at a higher temperature may tell a different story.

Another interesting finding is from the different springback behaviors between E-DSIF and E-SPIF strategies. As observed in Fig. 17, larger springback can be observed for the E-SPIF part during unclamping and trimming process while those of the E-DSIF part is much smaller. Considering that all the parts have similar shape and stiffness, the varied springback may imply different residual stresses resulted in the E-SPIF and E-DSIF processes: both E-DSIF processes may result in smaller residual stress than the E-SPIF process, which lead to the smaller springback. This reduced residual stress may be caused by the additional material deformation due to tool squeezing. However, further study on direct measuring the residual stress may be necessary to confirm this point. The reduced springback may also benefit the improvement of geometrical accuracy: if the springback is smaller, it will be much easier to compensate that geometric error by modifying the toolpath to reach higher accuracy.

Materials and Design 92 (2016) 268-280
http://dx.doi.org/10.1016/j.matdes.2015.12.009

7 Conclusion

The present study further investigated the main issues of the E-ISF approach in fabrication of lightweight alloys and explored the feasibility of E-DSIF in improving the part surface finish and geometrical accuracy. Moreover, a hybrid DSIF toolpath strategy has been developed to further enhance geometrical accuracy. The key findings from this investigation are outlined as follows:

(1) E-DSIF shows greater advantages than the E-SPIF process as the forming tool functions of taking load and serving as electrode can be separated.

(2) Although the roller-ball tool achieves better surface finish under large forming load, it cannot serve as an electrode at the same time. The rigid tool is a better option for the slave tool in E-DSIF.

(3) The developed hybrid DSIF toolpath strategy provides a feasible approach to eliminate the geometrical deviation due to bending.

(4) E-DISF could reduce the springback of finished parts during unclamping and trimming stages.

Acknowledgments

The authors are grateful for the financial support provided by National Key Specific Science & Technology Program from Ministry of Industry and Information Technology of China through Grant 2011ZX04016-051, and Marie Curie International Incoming Fellowship within 7th European Community Framework Programme (628055 & 913055).

References

[1] Jeswiet J, Micari F, Hirt G, Bramley A, Duflou J, Allwood J. Asymmetric Single Point Incremental Forming of Sheet Metal. CIRP Annals - Manufacturing Technology. 2005;54:88-114.

[2] Dittrich M, Gutowski T, Cao J, Roth J, Xia ZC, Kiridena V, et al. Exergy Analysis of Incremental Sheet Forming. Prod Eng. 2012;6:169-77.

[3] Ingarao G, Ambrogio G, Gagliardi F, Di Lorenzo R. A sustainability point of view on sheet metal forming operations: material wasting and energy consumption in incremental forming and stamping processes. Journal of Cleaner Production. 2012;29–30:255-68.

[4] Iseki H, Kato K, Sakamoto S. Flexible and incremental sheet metal forming using a spherical roller. In: Proc 40th JJCTP. 1989:41–4 (in Japanese).

[5] Matsubara S. Incremental Backward Bulge Forming of a Sheet Metal with a Hemispherical Head Tool. Journal of the JSTP. 1994;35:1311-6.

[6] Araghi BT, Manco GL, Bambach M, Hirt G. Investigation into a new hybrid forming process: Incremental sheet forming combined with stretch forming. CIRP Annals - Manufacturing Technology. 2009;58:225-8.

[7] Duflou JR, Verbert J, Belkassem B, Gu J, Sol H, Henrard C, et al. Process window enhancement for single point incremental forming through multi-step toolpaths. CIRP Annals - Manufacturing Technology. 2008;57:253-6.

[8] Meier H, Magnus C, Smukala V. Impact of superimposed pressure on dieless incremental sheet metal forming with two moving tools. CIRP Annals - Manufacturing Technology. 2011;60:327-30.

Materials and Design 92 (2016) 268-280
http://dx.doi.org/10.1016/j.matdes.2015.12.009

[9] Ji YH, Park JJ. Formability of magnesium AZ31 sheet in the incremental forming at warm temperature. Journal of Materials Processing Technology. 2008;201:354-8.
[10] Ambrogio G, Filice L, Manco GL. Warm incremental forming of magnesium alloy AZ31. CIRP Annals - Manufacturing Technology. 2008;57:257-60.
[11] Duflou JR, Callebaut B, Verbert J, De Baerdemaeker H. Laser Assisted Incremental Forming: Formability and Accuracy Improvement. CIRP Annals - Manufacturing Technology. 2007;56:273-6.
[12] Göttmann A, Bailly D, Bergweiler G, Bambach M, Stollenwerk J, Hirt G, et al. A novel approach for temperature control in ISF supported by laser and resistance heating. The International Journal of Advanced Manufacturing Technology. 2013;67:2195-205.
[13] Otsu M, Matsuo H, Matsuda M, Takashima K. Friction stir incremental forming of aluminum alloy sheets. Steel Research Internatoinal. 2010;81:942-5.
[14] Xu D, Wu W, Malhotra R, Chen J, Lu B, Cao J. Mechanism investigation for the influence of tool rotation and laser surface texturing (LST) on formability in single point incremental forming. International Journal of Machine Tools and Manufacture. 2013;73:37-46.
[15] Fan G, Gao L, Hussain G, Wu Z. Electric hot incremental forming: A novel technique. International Journal of Machine Tools and Manufacture. 2008;48:1688-92.
[16] Ambrogio G, Filice L, Gagliardi F. Formability of lightweight alloys by hot incremental sheet forming. Materials & Design. 2012;34:501-8.
[17] Palumbo G, Brandizzi M. Experimental investigations on the single point incremental forming of a titanium alloy component combining static heating with high tool rotation speed. Materials & Design. 2012;40:43-51.
[18] Xu D, Lu B, Cao T, Chen J, Long H, Cao J. A Comparative Study on Process Potentials for Frictional Stir- and Electric Hot-assisted Incremental Sheet Forming. Procedia Engineering. 2014;81:2324-9.
[19] Cao J, Roth JT, Xia C, Gutowski T. A Hybrid Forming System: Electrical-Assisted Double Side Incremental Forming (EADSIF) Process for Enhanced Formability and Geometrical Flexibility. Report to DOE/EERE - Industrial Technologies Program, 8pp, October 2010. 2010.
[20] Meier H, Magnus C. Incremental Sheet Metal Forming with Direct Resistance Heating Using Two Moving Tools. Key Engineering Materials. 2013;554-557:1362-7.
[21] Asgar J, Lingam R, Reddy NV. Tool path influence on electric pulse aided deformation during incremental sheet metal forming The 9th International Conference and Workshop on Numerical Simulation of 3D Sheet Metal Forming Prcesses. Melbourne, Australia2014. p. 840-3.
[22] Malhotra R, Cao J, Beltran M, Xu D, Magargee J, Kiridena V, et al. Accumulative-DSIF strategy for enhancing process capabilities in incremental forming. CIRP Annals - Manufacturing Technology. 2012;61:251-4.
[23] Malhotra R, Cao J, Ren F, Kiridena V, Cedric Xia Z, Reddy NV. Improvement of Geometric Accuracy in Incremental Forming by Using a Squeezing Toolpath Strategy With Two Forming Tools. Journal of Manufacturing Science and Engineering. 2011;133:061019.
[24] Kim YH, Park JJ. Effect of process parameters on formability in incremental forming of sheet metal. Journal of Materials Processing Technology. 2002;130–131:42-6.
[25] Hussain G, Gao L, Hayat N, Cui Z, Pang YC, Dar NU. Tool and lubrication for negative incremental forming of a commercially pure titanium sheet. Journal of Materials Processing Technology. 2008;203:193-201.
[26] Fan G, Sun F, Meng X, Gao L, Tong G. Electric hot incremental forming of Ti-6Al-4V titanium sheet. The International Journal of Advanced Manufacturing Technology. 2010;49:941-7.
[27] Zhang Q, Xiao F, Guo H, Li C, Gao L, Guo X, et al. Warm negative incremental forming of magnesium alloy AZ31 Sheet: New lubricating method. Journal of Materials Processing Technology. 2010;210:323-9.
[28] Tekkaya A, Shankar R, Sebastiani G, Homberg W, Kleiner M. Surface reconstruction for incremental forming. Computer Aided Engineering. 2007;1:71-8.
[29] Micari F, Ambrogio G, Filice L. Shape and dimensional accuracy in Single Point Incremental Forming: State of the art and future trends. Journal of Materials Processing Technology. 2007;191:390-5.
[30] Han F, Mo JH, Cui XH, Wang ZL. Studies on the Springback Mechanism of Incremental Sheet Forming Based on FEM Simulation. Advanced Materials Research. 2010;102-104:242-6.
[31] Ruszkiewicz B, Dodds SS, Reese ZC, Roth JT, Ragai I. Incrementally Formed Stiffeners Effect on the Reduction of Springback in 2024-T3 Aluminum After Single Point Incremental Forming ASME 2015 International Manufacturing Science and Engineering Conference. Charlotte, US.2015. p. 9437.

Materials and Design 92 (2016) 268-280
http://dx.doi.org/10.1016/j.matdes.2015.12.009

[32] Ruszkiewicz B, Johnson DH, Roth JT. Locally Applied Direct Electric Current's Effect on Springback of 2024-T3 Aluminum After Single Point Incremental Forming. ASME 2015 International Manufacturing Science and Engineering Conference. Charlotte, US2015. p. 9429.
[33] Ren F, Xia C. Method to improve geometrical accuracy of an incrementally formed workpiece US Patent, US 8783078 B22010.
[34] Shi X, Gao L, Khalatbari H, Xu Y, Wang H, Jin L. Electric hot incremental forming of low carbon steel sheet: accuracy improvement. The International Journal of Advanced Manufacturing Technology. 2013;68:241-7.
[35] Malhotra R, Bhattacharya A, Kumar A, Reddy NV, Cao J. A new methodology for multi-pass single point incremental forming with mixed toolpaths. CIRP Annals - Manufacturing Technology. 2011;60:323-6.
[36] Silva MB, Skjoedt M, Atkins AG, Bay N, Martins PAF. Single-point incremental forming and formability/failure diagrams. Journal of Strain Analysis. 2008;43:15–36.
[37] Emmens WC, Boogaard AH. An overview of stabilizing deformation mechanisms in incremental sheet forming. Journal of Materials Processing Technology. 2009;209:3688-95.
[38] Zhang Q, Guo H, Xiao F, Gao L, Bondarev AB, Han W. Influence of anisotropy of the magnesium alloy AZ31 sheets on warm negative incremental forming. Journal of Materials Processing Technology. 2009;209:5514-20.
[39] Taleb Araghi B, Göttmann A, Bergweiler G, Saeed-Akbari A, Bültmann J, Zettler J, et al. Investigation on Incremental Sheet Forming Combined with Laser Heating and Stretch Forming for the Production of Lightweight Structures. Key Engineering Materials. 2011;473:919-28.
[40] Sy LV, Nam NT. Hot incremental forming of magnesium and aluminum alloy sheets by using direct heating system. Proceedings of the Institution of Mechanical Engineers Part B-J Eng Manuf. 2013;227:1099-110.
[41] Lu B, Fang Y, Xu DK, Chen J, Ou H, Moser NH, et al. Mechanism investigation of friction-related effects in single point incremental forming using a developed oblique roller-ball tool. International Journal of Machine Tools and Manufacture. 2014;85:14-29.
[42] Lu B, Chen J, Ou H, Cao J. Feature-based tool path generation approach for incremental sheet forming process. Journal of Materials Processing Technology. 2013;213:1221-33.